

Journal of Materials Chemistry C

Accepted Manuscript



This is an *Accepted Manuscript*, which has been through the Royal Society of Chemistry peer review process and has been accepted for publication.

Accepted Manuscripts are published online shortly after acceptance, before technical editing, formatting and proof reading. Using this free service, authors can make their results available to the community, in citable form, before we publish the edited article. We will replace this *Accepted Manuscript* with the edited and formatted *Advance Article* as soon as it is available.

You can find more information about *Accepted Manuscripts* in the [Information for Authors](#).

Please note that technical editing may introduce minor changes to the text and/or graphics, which may alter content. The journal's standard [Terms & Conditions](#) and the [Ethical guidelines](#) still apply. In no event shall the Royal Society of Chemistry be held responsible for any errors or omissions in this *Accepted Manuscript* or any consequences arising from the use of any information it contains.

Graphene Aerogel Composites Derived From Recycled Cigarette Filter for Electromagnetic Wave Absorption

Chunhui Wang,¹ Yujie Ding,¹ Ye Yuan,¹ Xiaodong He,^{1*} Shiting Wu,² Song Hu,²

Mingchu Zou,² Wenqi Zhao,¹ Liusi Yang,² Anyuan Cao,² Yibin Li,^{1*}

¹Center for Composite Materials and Structures, Harbin Institute of Technology, Harbin 150080, P. R. China

²Department of Materials Science and Engineering, College of Engineering, Peking University, Beijing 100871, P. R. China

*Corresponding authors. Email: liyibin@hit.edu.cn, hexd@hit.edu.cn

Abstract

Assembling graphene nanosheets into three dimensional aerogels has attracted considerable interest due to their unique properties and potential applications in many fields. Here, graphene aerogels constructed by interconnected graphene nanosheets coated-carbon fibers are fabricated by using cigarette filters as the template via a simple dip-coating method. The composite aerogels are ultralight ($\rho = 7.6 \text{ mg cm}^{-3}$) yet have high mechanical strength (0.07 MPa); when used as electromagnetic wave absorber, they showed a minimum reflection loss value of -30.53 dB at 14.6 GHz and the bandwidth of reflection loss less than -10 dB (90% absorption) is 4.1 GHz. Furthermore, coating polypyrrole into the composite aerogels can increase the minimum reflection loss value to -45.12 dB. Our results provide a promising approach to fabricate graphene-based composite aerogels with strong electromagnetic wave absorption ability.

Keywords: cigarette filter, graphene aerogel, carbon fibers, electromagnetic wave.

Introduction

With the rapid development of wireless technology, digital devices and radar system, electromagnetic (EM) interference and radiation have become severe pollution sources because of their impacts on both humans and the environment.^[1-3] To solve these problems, one effective method is to use microwave absorption materials to attenuate those unwanted EM energies.^[4, 5] Thus, much effort has been devoted to the development of high-performance EM absorbents. An EM absorbent is a type of functional material that is able to absorb incidence of EM wave effectively and then attenuate it in the form of thermal energy.^[6, 7] Ideal absorbents must be lightweight, as well as exhibit strong absorption, high thermal stability, and a broad absorption frequency bandwidth.^[8, 9] To this end, several materials such as metals,^[2, 4] carbon fibers (CFs),^[10-12] carbon nanotubes (CNTs),^[13, 14] graphene^[15-18] and conducting polymers^[19-21] have been investigated. Among them, carbon-based materials and their composites have been found to be effective candidates owing to their excellent mechanical and electrical properties.

As a conventional EM absorbing material, a great deal of research on CFs has been conducted. Porous CFs prepared from polyacrylonitrile/polymethylmethacrylate showed a minimum reflection loss (RF_m) of -31 dB at 9.7 GHz.^[10] In another report, modified CFs grafted with magnetite (Fe_3O_4) nanoparticles and CNTs had been proven that the RF_m can reach up to -50.9 dB at 14.03 GHz.^[11] Despite their outstanding performance on EM absorption, however, one dimensional CFs need to be fabricated into shaped woven fabrics and then embedded into polymer matrix for further use because of their inconvenient manipulation.^[12]

Recently, carbon foams found their way to act as EM absorbers due to their light-weight, easy manipulation and effective EM wave absorbing capability.^[22] Graphene aerogels (GAs), a new-generation carbon foam, are highly porous three-dimensional (3D) networks constructed by interconnected graphene sheets have especially attracted tremendous attention. The high surface area and strong dielectric

loss of GAs indicate that they are good candidates for EM absorbers.^[23, 24] Also, the 3D skeleton of GAs makes it possible to synthesize multifunctional GAs by introducing functional nanofillers. The composite aerogels will inherit the properties from graphene and nanofillers as well as provide enhanced new properties owing to the interaction between individual patents.^[25, 26] For example, zinc oxide (ZnO)/graphene hybrid aerogel could exhibit an excellent RF_m up to -25.95 dB due to the synergetic effect of ZnO and graphene sheets.^[27] By adding α -Fe₂O₃ nanoparticles into GAs, the effective bandwidths of this composite was 7.12 GHz and the RF_m was -33.5 dB.^[28] Moreover, the RF_m of thermally treated Polyvinyl alcohol/graphene GAs reached to -43.5 dB at 12.19 GHz because of the enhanced conductivity by carbonization.^[29] This development of novel functional graphene aerogels may pave the way for practical applications in EM absorption.

Herein, we fabricate high EM absorption GAs composed of CFs and graphene nanosheets, and the composite aerogels are lightweight yet with high mechanical strength. Our basic idea is to use cigarette filter, a non-biodegradable residual waste mainly composed of cellulose acetate (CA), as the scaffold of the composite aerogel while graphene oxide nanosheets (GO) were coated on them in the form of core-shell structures; after thermal annealing, the cellulose fibers were carbonized into CFs and also GO sheets were reduced simultaneously. The all-carbon CF@G aerogels are robust with a compressive strength of ~ 0.07 MPa (much higher than previous reported GAs). The EM absorption capacity of the bare CF@G is -30.53 dB at 14.6 GHz. When they were coated with polypyrrole, a conducting polymer usually used for EM absorption, the RF_m was further improved to -45.12 dB at 7.9 GHz.

Results and discussion

The cigarette filters played an important role in the fabrication process and were used as structural template for the synthesis of our composite aerogels (Scheme 1). Each of them composed of aligned CA arrays (Fig. 1a), somewhat like the CNT forest, although CA have a larger size in macroscopic level (about 4 centimeter in length and 20 μ m in diameter for each CA fibers). After soaked in GO solution for a certain time,

these GO coated-celluloses (CA@GO) were subjected to thermal annealing for the carbonization of celluloses fibers into CFs and the reduction of GO into graphene. Then, composite aerogels consist of interconnected graphene nanosheets-wrapped CFs were formed (CF@G). It is noted that cigarette filters without graphene coatings cannot form the 3D structure under the same synthesis condition; instead, they were carbonized into carbon ashes (Supporting Information, Fig. S1), indicating the synergetic effect of the graphene nanosheets. The layer of GO coated on the backbone of cigarette filters helped to keep the cylindrical shape of the templates. Furthermore, CF@G aerogel was coated with pyrrole monomers and immersed into FeCl₃ solution for polymerization into the CF@G@PPy aerogels with enhanced properties (Scheme 1) for further use.

Compared with pristine cigarette filter, the height of CF@G decreased from 3 cm to 1.9 cm and the diameter decreased from 8 mm to 6.9 cm. The volume of CF@G aerogel is thus only ~ 47 % of that of cigarette filter (Fig. 2a). The CF@G aerogel has a low density of ~ 7.6 mg cm⁻³ and CF@G@PPy is slightly larger (~ 8.8 mg cm⁻³) due to the addition of PPy, thus both of them belong to the ultralight materials category (< 10 mg cm⁻³). The morphologies of CF@G and CA@GO were characterized by scanning electron microscopy (SEM). Images of the top view and side view of both samples are shown in Fig. 1a-d. Relatively ordered fibers are observed for CA@GO (Fig. 1a), however, the fibers are cross-linked and twisted for CF@G (Fig. 1b) owing to carbonization. The pore sizes of CF@G range from 100-300 μm were observed in the cross-section images along the axis (Fig. 1d), which are larger than CA@GO due to the shrinkage of the CA fibers. The pristine CA fibers displayed a “Y”-shape cross-section with the diameter of ~ 20 μm (Fig. 1e), while after annealing at 900 °C the fibers shrank into ~ 5 μm in diameter with thick graphene layers on the surface (Fig. 1f). The fibers are connected together to form a piece by the connection of graphene nanosheets and amplified SEM image reveals that the graphene nanosheets are strongly adhered to the CF like leaves grown on a trunk (Fig. S1), and the leaves become thicker when they were coated with PPy (Fig. S2).

A burning experiment was carried out on an alcohol lamp for CF@G and CA@GO (Fig. 2a), the CA@GO sample was easily ignited and melted while CF@G exhibited a good thermal stability against burning which is beneficial for using as EM absorption materials. Despite the low density, a CF@G aerogel is robust enough to sustain 4,000 times its own weight without collapse (Fig. 2a). The cross-linked graphene-coated fibers enhanced the integral strength of our composite aerogels. Although there is a decrease in mechanical strength compared with CA@GO owing to the carbonization (Fig. S3), our CF@G aerogel still exhibit a high strength of 0.07 Mpa (Fig. 2b) which is higher than previously reported graphene aerogels (Table S1). The CF@G@PPy exhibit a higher value up to 0.09 Mpa due to the PPy layers. The enhanced mechanical strength is attributed to the synergetic effect of the CF and the graphene nanosheets. Here, CF serves as the composite matrix while graphene nanosheets are the nanofillers. When a lower concentration GO was used, the strength of CF@G decreased correspondingly (Fig. 2b). Chemical analysis was also conducted by Fourier Translation Infrared Spectroscopy (FT-IR). Spectrum of pure CA shows characteristic peaks at 1740, 1367 and 1220 cm^{-1} regard to the C=O, C-CH₃ and C-O-C stretching, respectively. After being coated with GO and carbonized, all these peaks vanished leaving the C=C stretching peak (1620 cm^{-1}), reflecting the removal of oxygen contained groups during carbonization. Some new peaks rise (1544.4 cm^{-1}) in the spectrum of CF@G@PPy due to the pyrrole ring vibration and C-N stretching vibration (1290.9 cm^{-1}). The peaks at 1456.1 cm^{-1} , 1385.3 cm^{-1} , 896.6 cm^{-1} and 783 cm^{-1} correspond to the =C-H in-plane vibration and the =C-H out-of-plane vibration of the pyrrole ring. To further characterize the physical properties of CF@G aerogels, N₂ adsorption/desorption analysis was performed and the results indicate the high surface area of CF@G with the value of 264 $\text{m}^2 \text{g}^{-1}$; the pores of our aerogels are larger than 5 nm and have a wide size distribution from 5 nm to 20 nm (Fig. 2d). The porous structure of our aerogel is suitable for EM adsorption because the EM wave can easily enter into the inside of CF@G aerogels with less reflectivity. Also, X-ray photoelectron spectroscopy (XPS) analysis was conducted to investigate the element distribution of our aerogels (Fig. S4). After thermal annealing, the C_{1s} peak of CF@G

aerogels increased dramatically indicating the reduction of GO and carbonization of cellulose fibers and the nitrogen atoms content is ~ 8.5 wt% after they were coated with PPy.

To study the EM absorbing properties, our aerogels were impregnated with paraffin wax and fabricated into cylindrical specimens (Fig. S5). According to the EM energy conversion principle, the reflection and attenuation characteristics of EM absorbents are determined by the relative complex permittivity ($\epsilon_r = \epsilon' - j\epsilon''$), relative complex permeability ($\mu_r = \mu' - j\mu''$) and proper matching between ϵ_r and μ_r . Considering that no ferromagnetic materials were involved in our samples, here the complex permeability was taken as 1 ($\mu_r = 1$).^[30] The complex permittivity values (ϵ_r) were measured in the frequency range of 2-18 GHz (Fig. S6). The real part (ϵ') and imaginary part (ϵ'') of complex permittivity represent the stored electrical energy within the medium and the dissipation (or loss) of the electrical energy, respectively. Thus, a high value of ϵ'' means strong dielectric loss to EM wave. As shown in Fig. S6, the permittivity values increase with higher loading of aerogel samples in wax owing to better conductivity. All samples show typical frequency dependent permittivity, when the frequency increases in the measured region both ϵ' and ϵ'' are found to decrease, probably due to the resonance behavior. The CF@G@PPy exhibits some typical dielectric resonances at 8-16 GHz, especially for the ϵ'' (\sim at 8, 10, 12, 14 GHz) while such phenomenon is absent for the CF@G samples. It is clearly seen that overall the ϵ' value of CF@G@PPy are larger than CF@G. However, the ϵ'' of CF@G@PPy is slightly lower than that of CF@G in the range of 2.0-9.0 GHz (Fig. S6f). This behavior is due to the interfacial polarization and associated relaxation at the interfaces between the PPy core, graphene core and the CF shell.^[31, 32]

The dielectric tangent loss ($\tan \delta_E = \epsilon''/\epsilon'$) provide a measure of the power lost in a material versus the amount of power stored and higher values of $\tan \delta_E$ indicate more EM energy will be consumed (Fig. 3a,b). For CF@G aerogels, $\tan \delta_E$ increase with increasing loadings in wax. The $\tan \delta_E$ for 20 wt% of CF@G in wax ranges from 0.46 to 0.65 with a maximum value of 0.83 at 11.7 GHz. CF@G@PPy aerogels have the same trend with increasing loadings in wax with $\tan \delta_E$ range from 0.28-0.62 (20

wt%), and three peaks rise at the range of 11.8, 14 and 16GHz with corresponding value of 0.89, 0.86 and 0.78, respectively. However, at 12-15 GHz 15 wt% CF@G@PPy in wax is higher than 20 wt% samples, which indicates that these samples exhibit higher loss capabilities for electric energy at this bandwidth. This permittivity behavior can be attributed to the increase of electric conductivity and space-charge polarization among PPy layers isolated by the wax matrix. Several factors should be considered in order to obtain an ideal reflection loss (RL (dB)), such as magnetic loss, dielectric loss, characteristic impedance, interface relaxation, etc. Debye dipolar relaxations are also favorable for the enhancement of dielectric loss materials to absorb EM waves. According to Debye theory, the complex permittivity (ϵ_r) can be written as,

$$\epsilon_r = \epsilon' + i\epsilon'' = \epsilon_\infty + \frac{\epsilon_s - \epsilon_\infty}{1 + i\omega\tau_0} \quad (1)^{[8]}$$

Where ϵ_s is the static dielectric constant, ϵ_∞ is the dielectric constant at infinite frequency and τ_0 is the relaxation time. The equation (1) can be deduced into:

$$\epsilon' = \epsilon_\infty + \frac{\epsilon_s - \epsilon_\infty}{1 + (\omega\tau_0)^2} \quad (2)$$

$$\epsilon'' = \frac{\omega\tau_0(\epsilon_s - \epsilon_\infty)}{1 + (\omega\tau_0)^2} \quad (3)$$

The relationship between ϵ' and ϵ'' can be deduced from equation (2) and (3) as follows:

$$(\epsilon' - \epsilon_\infty)^2 + (\epsilon'')^2 = (\epsilon_s - \epsilon_\infty)^2 \quad (4)$$

Therefore, the plot of ϵ' versus ϵ'' would be a single semicircle, generally denoted as the Cole-Cole semicircle.^[30] Each semicircle corresponds to a Debye dipolar relaxation. As shown in Fig. 3d, at least three semicircles were found in the curves of CF@G@PPy (20 wt% in wax) compared with CF@G (20 wt% in wax) with only one semicircle (Fig. 3c) in the range of 2-18 GHz, indicating the PPy coatings endows CF@G@PPy with multiple dielectric relaxation processes. The residual oxygen functional groups such as hydroxyl (-OH), epoxy (C-O-C) and carbonyl groups (C=O) in the thermally reduced graphene and the amino groups (N-H) in the PPy molecular act as the polarized centers which account for the presence of higher EM wave absorption.

To further evaluate the EM absorption performance of CF@G and CF@G@PPy aerogels, we calculated the RL values at a given frequency and absorber thickness. When the RL is below -10 dB, only 10% of the EM power was reflected and 90% of the EM energy was absorbed. Fig. 4b, c shows the RL values of samples (20 wt% in wax) with different thicknesses at 2-18 GHz. The minimum RF (RF_m) shifts towards a lower frequency with increasing thickness, owing to the phenomena of quarter-wavelength attenuation, which can be explained by the quarter-wavelength equation^[3]:

$$t_m = \frac{n\lambda}{4} = \frac{nc}{4f_m\sqrt{|\mu_r||\epsilon_r|}} \quad (n=1, 3, 5, \dots) \quad (5)$$

Where t_m is the thickness of absorber, λ is the wavelength of the electromagnetic wave, f_m is the peak frequency of the maximum RL, $|\mu_r|$ and $|\epsilon_r|$ are respectively the modulus of the measured μ_r and ϵ_r at f_m , and c is the velocity of light in a vacuum. The RL_m of CF@G is -30.53 dB at 14.6 GHz when the thickness is 1.5 mm, and the bandwidth of RL values less than -10 dB is 4.1 GHz (from 12.7-16.8 GHz). When the filler loadings decrease, the absorption decreases correspondingly (15 wt%, 10 wt% and 5% wt% can be seen in Fig. S7). The reflection loss properties toward incident EM waves of CF@G@PPy are enhanced substantially. The RL_m of CF@G@PPy (20 wt % in wax) is -45.12 dB at 7.9 GHz with the thickness of 2.5 mm. The bandwidth of RL below -10 dB at this thickness is 2.5 GHz (from 6.9-9.4 GHz). CF@G@PPy with other thicknesses also exhibit excellent EM absorption, the RL_m of 1.5 mm, 2.0 mm and 3.0mm are -35.95 dB, -42.33 dB and -40.59 dB, and the bandwidths exceeding -10 dB for these samples are 13.2-16.9 GHz, 9.2-12.6 GHz and 5.6-7.4 GHz, respectively. Moreover, it is clear to see that the RL below -10 dB for both CF@G and CF@G@PPy can be obtained in the range of 2-18 GHz with a variation in thickness from 1.5 to 5.0 mm, indicating excellent EM absorption of our aerogels. To shed light on the EM absorption mechanism of our aerogels, Fig. 4a schematically depicts the EM transfer across our aerogels. The entered microwaves are trapped in the composite aerogels and attenuated by scattering between the fibers. The EM waves are hard to escape from the trap until being absorbed and dissipated as heat.^[33]

We further investigated the influence of PPy content on the EM absorption of CF@G@PPy samples. Two other CF@G@PPy samples with higher PPy content (46.5 wt% and 70 wt%, respectively.) were fabricated. However, the EM absorption decreases with increasing PPy content. The RL_m of CF@G@PPy-46.5 wt% is -34.2 dB at 14.5 GHz at the thickness of 2 mm and the bandwidth of RL below -10 dB is 4.3 GHz (11.9-16.2 GHz), as Fig. 5a shows. When the PPy content reaches 70 wt%, the RL_m CF@G@PPy-70 wt% is only -22.8 dB at 17.9 GHz (Fig. 5b). And only samples with thicknesses of 4.0, 4.5 and 5.0 mm have EM absorption below -10 dB at a small bandwidth (15-18 GHz). As we have discussed before, there are many factors to be considered in order to achieve ideal EM absorption. Too much PPy layers coated on CF@G aerogel will increase the conductivity of the aerogels; this could decrease the dielectric properties of the composite aerogels and affect the impedance match, which would lower the reflection loss. Most of the EM waves are reflected rather than absorbed at this situation, thus, resulting in a decrease in EM absorption. Therefore, CF@G composite aerogels with different EM wave absorption performance can be obtained by adjusting the proportion of PPy (Fig. 5c). To better understand the EM absorption capacity of our aerogels, we made comparisons between our aerogels and other reported graphene-based aerogels (Fig. 5d, Table S2). The results show that our aerogels are excellent EM absorbers with RL_m can reach -45.12 dB for CF@G@PPy samples (others range from -22 to -43.5 dB) among all these samples and the effective bandwidth of our aerogel is also perfect with a value of 4.1 GHz for CF@G samples, and this may develop new broadband EM absorbing materials.

Conclusions

We have synthesized ultralight yet high mechanical strength 3D porous composite graphene aerogels by using cigarette filters as templates via a solution coating method. Our composite aerogels have presented strong EM wave absorption abilities (minimum $RL = -30.53$ dB) and wide absorption bandwidths (4.1 GHz). After coated with conducting polymer polypyrrole by a simple chemical polymerization method, the minimum RL can reach up to -45.12 dB. The easy fabrication process and

environmentally friendly raw materials make our aerogels good candidates for application in EM wave absorption.

Acknowledgements

Y. Li and X. He acknowledge the Natural Science Foundation in China (NSFC 11272109) and the Ph. D. Programs Foundation of Ministry of Education of China (20122302110065).

Experimental

Synthesis of CF@G Aerogel

Waste cigarette filters were collected and the wrapping papers were removed. The cellulose acetate filters were rinsed and then immersed into GO suspension (10 mg mL^{-1}) for 2 h until the GO adsorption was saturated. The resulting CA@GO composites were then dried in air at room temperature overnight. Finally, CA@GO composites were subjected to thermal annealing at $900 \text{ }^\circ\text{C}$ for 2 h in Ar and the production was named as CF@G aerogel.

Fabrication of CF@G@PPy Aerogel

CF@G aerogel was immersed in pyrrole solution for 1 h. Then CF@G aerogel with Py monomers adsorbed on the surface was directly immersed in FeCl_3 (1 M) for 15 min, followed by rinsing with deionized water. Then, samples were dried in air. The PPy content is about 18.5 wt%.

For comparison, samples with 46.5 wt% and 70 wt% PPy were also fabricated by extending the reaction time in FeCl_3 solution to 30 min and 1 h, respectively.

Materials Measurements

Mechanical tests were carried out by a single-column static instrument (Instron 5843) equipped with two flat-surface compression stages and a 10 N load cell. For electromagnetic wave absorption measurements, our aerogels were impregnated with paraffin wax at $85 \text{ }^\circ\text{C}$ and then fabricated into cylindrical specimens. Paraffin wax was used as a matrix to support aerogels and facilitate the sample fabrication process. The wax is transparent to EM waves and makes no contribution to EM absorption. Samples with different aerogel loadings in the paraffin wax were fabricated, such as 20 wt%, 15 wt%, 10 wt% and 5 wt% and then the resulting paraffin composites were compressed into cylindrical specimens with an inner diameter of 3 mm, outer diameter of 7 mm. The complex permittivity ($\epsilon_r = \epsilon' - j\epsilon''$) and relative complex permeability ($\mu_r = \mu' - j\mu''$) were measured using the T/R coaxial line method in the range of 2-18 GHz using a network analyzer (Agilent Technologies N5230A). The reflection loss (RL) curves calculated from the following equations:

$$RL (dB) = 20 \log \left| \frac{Z_{in}-1}{Z_{in}+1} \right| \quad (6)$$

Where Z_{in} is the normalized input impedance of the microwave absorption layer, which can be written as the following equation:

$$Z_{in} = \sqrt{\frac{\mu_r}{\epsilon_r}} \tanh \left[j \frac{2\pi}{c} \sqrt{\mu_r \epsilon_r} f d \right] \quad (7)$$

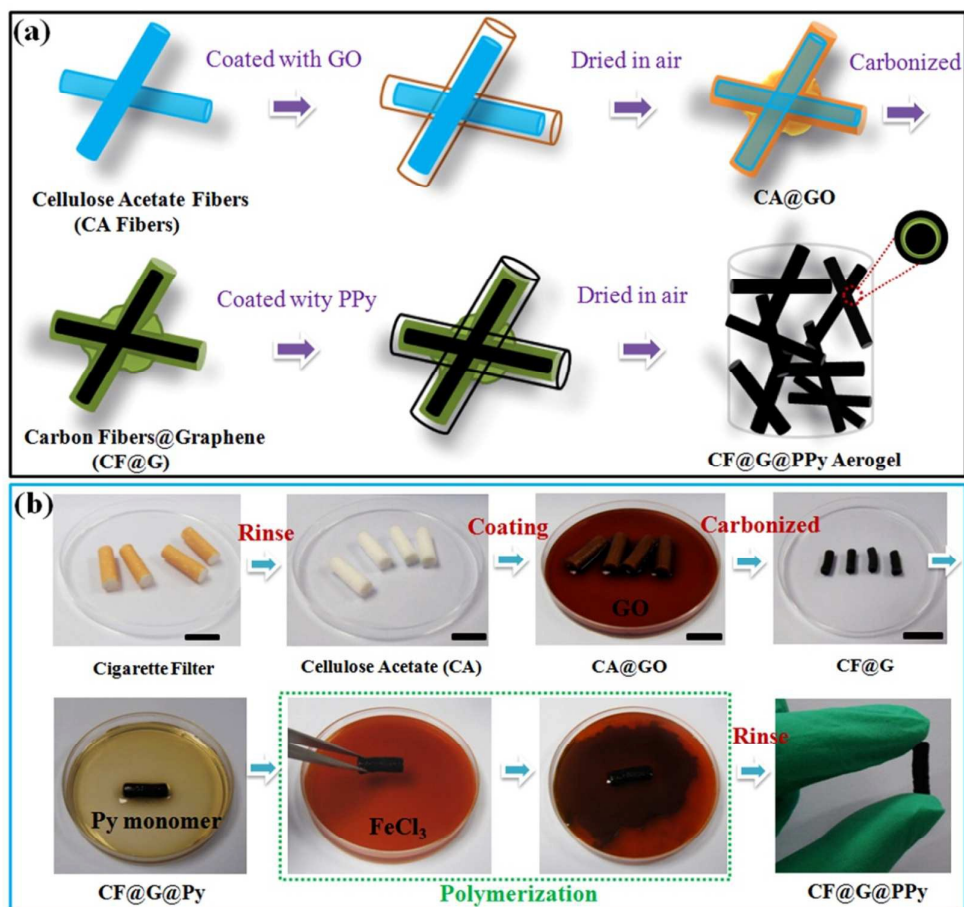
Where c is the velocity of light in a vacuum, f is the microwave frequency, d is the thickness of the absorber, ϵ_r and μ_r are the relative permittivity and permeability of the materials. In this paper the complex permeability was taken as 1 because of the weak magnetic properties of our samples.

References

- [1] Zhang, X. F.; Guo, J. J.; Qin, G. W. Assembled Micro-nano Particles with Multiple Interface Polarizations for Electromagnetic Absorption at Gigahertz. *Appl. Phys. Lett.* **2014**, *104*, 252404.
- [2] Lv, H. L.; Liang, X. H.; Cheng, Y.; Zhang, H. Q.; Tang, D. M.; Zhang, B. S.; Ji, G. B.; Du, Y. W. Coin-like α -Fe₂O₃@CoFe₂O₄ Core-Shell Composites with Excellent Electromagnetic Absorption Performance. *ACS Appl. Mater. Interfaces* **2015**, *7*, 4744-4750.
- [3] Lv, H. L.; Liang, X. H.; Ji, G. B.; Zhang, H. Q.; Du, Y. W. Porous Three-Dimensional Flower-like Co/CoO and Its Excellent Electromagnetic Absorption Properties. *ACS Appl. Mater. Interfaces* **2015**, *7*, 9776-9783.
- [4] Kumar, A.; Singh, A. P.; Kumari, S.; Dutta, P. K.; Dhawan, S. K.; Dhar, A. Polyaromatic-Hydrocarbon-Based Carbon Copper Composites for the Suppression of Electromagnetic Pollution. *J. Mater. Chem. A* **2014**, *2*, 16632-16639.
- [5] Zhang, D. F.; Xu, F. X.; Lin, J.; Yang, Z. D.; Zhang, M. Electromagnetic Characteristics and Microwave Absorption Properties of Carbon-Encapsulated Cobalt Nanoparticles in 2-18 GHz Frequency Range. *Carbon* **2014**, *80*, 103-111.
- [6] Lv, Y. Y.; Wang, Y. T.; Li, H. L.; Lin, Y.; Jiang, Z. Y.; Xie, Z. X.; Kuang, Q.; Zheng, L. S. MOF-Derived Porous Co/C Nanocomposites with Excellent Electromagnetic Wave Absorption Properties. *ACS Appl. Mater. Interfaces* **2015**, *7*, 13604-13611.
- [7] Li, G.; Wang, L.; Li, W.; Ding, R.; Xu, Y. CoFe₂O₄ and/or Co₃Fe₇ Loaded Porous Activated Carbon Balls as Lightweight Microwave Absorbent. *Phys. Chem. Chem. Phys.* **2014**, *16*, 12385-12392.
- [8] Du, Y. C.; Liu, W. W.; Qiang, R.; Wang, Y.; Han, X. J.; Ma, J.; Xu, P. Shell Thickness-Dependant Microwave Absorption of Core-Shell Fe₃O₄@C Composites. *ACS Appl. Mater. Interfaces* **2014**, *6*, 12997-13006.
- [9] Chen, Z.; Xu, C.; Ma, C.; Ren, W.; Cheng, H. M. Lightweight and Flexible Graphene Foam Composites for High-Performance Electromagnetic Interference Shielding. *Adv. Mater.* **2013**, *25*, 1296-1300.
- [10] Li, G.; Xie, T.; Yang, S.; Jin, J.; Jiang, J. Microwave Absorption Enhancement of Porous Carbon Fibers Compared with Carbon Nanofibers. *J. Phy. Chem. C* **2012**, *116*, 9196-9201.
- [11] Qiu, J.; Qiu, T. T. Fabrication and Microwave Absorption Properties of Magnetite Nanoparticle-Carbon Nanotube-Hollow Carbon Fiber Composites. *Carbon* **2015**, *81*, 20-28.
- [12] Cao, M. S.; Song, W. L.; Hou, Z. L.; Wen, B.; Yuan, J.; The Effects of Temperature and Frequency on the Dielectric Properties, Electromagnetic Interference Shielding and Microwave-absorption of Short Carbon Fiber/Silica Composites. *Carbon* **2010**, *48*, 788-796.
- [13] Yang, Y. L.; Gupta, M. C. Novel Carbon Nanotube-Polystyrene Foam Composites for Electromagnetic Interference Shielding. *Nano Lett.* **2005**, *5*, 2131-2134.
- [14] Lu, M. M.; Cao, M. S.; Chen, Y. H.; Cao, W. Q.; Liu, J.; Shi, H. L.; Zhang, D. Q.; Wang, W. Z.; Yuan, J. Multiscale Assembly of Grape-Like Ferroferric Oxide and Carbon Nanotubes: A Smart Absorber Prototype Varying Temperature to Tune Intensities. *ACS Appl. Mater. Interfaces* **2015**, *7*, 19408-19415.

- [15] Wen, B.; Cao, M.; Lu, M.; Cao, W.; Shi, H.; Liu, J.; Wang, X.; Jin, H.; Fang, X.; Wang, W.; Yuan, J. Reduced Graphene Oxides: Light-Weight and High-Efficiency Electromagnetic Interference Shielding at Elevated Temperatures. *Adv. Mater.* **2014**, *26*, 3484-3489.
- [16] Yousefi, N.; Sun, X. Y.; Lin, X. Y.; She, X.; Jia, J. J.; Zhang, B.; Tang, B. Z.; Chan, M. S.; Kim, J. K. Highly Aligned Graphene/Polymer Nanocomposites with Excellent Dielectric Properties for High-Performance Electromagnetic Interference Shielding. *Adv. Mater.* **2014**, *26*, 5480-5487.
- [17] Wang, L.; Huang, Y.; Sun, X.; Huang, H. J.; Liu, P. B.; Zong, M.; Wang, Y. Synthesis and Microwave Absorption Enhancement of Graphene @ Fe₃O₄@SiO₂@NiO Nanosheet Hierarchical Structures. *Nanoscale* **2014**, *6*, 3157-3164.
- [18] Sun, D.; Zou, Q.; Wang, Y.; Wang, Y.; Jiang, W.; Li, F. Controllable Synthesis of Porous Fe₃O₄@ZnO Sphere Decorated Graphene for Extraordinary Electromagnetic Wave Absorption. *Nanoscale* **2014**, *6*, 6557-6562.
- [19] Joo, J.; Lee, C. Y. J. High Frequency Electromagnetic Interference Shielding Response of Mixtures and Multilayer Films Based on Conducting Polymers. *Appl. Phys.* **2000**, *88*, 513-518.
- [20] Xie, A. M.; Wu, F.; Sun, M. X.; Dai, X. Q.; Xu, Z. H.; Qiu, Y. Y.; Wang, Y.; Wang, M. Y. Self-Assembled Ultralight Three-Dimensional Polypyrrole Aerogel for Effective Electromagnetic Absorption. *Appl. Phys. Lett.* **2015**, *106*, 222902.
- [21] Zhao, J.; Lin, J. P.; Xiao, J. P.; Fan, H. L. Synthesis and Electromagnetic, Microwave Absorbing Properties of Polyaniline/Graphene Oxide/Fe₃O₄ Nanocomposites. *RSC Adv.* **2015**, *5*, 19345-19352.
- [22] Fang, Z.; Li, C.; Sun, J.; Zhang, H.; Zhang, J. The Electromagnetic Characteristics of Carbon Foams. *Carbon* **2007**, *45*, 2873-2879.
- [23] Shen, B.; Zhai, W. T.; Tao, M. M.; Ling, J. Q.; Zheng, W. G. Lightweight, Multifunctional Polyetherimide/Graphene@Fe₃O₄ Composite Foams for Shielding of Electromagnetic Pollution. *ACS Appl. Mater. Interfaces* **2013**, *5*, 11383-11391.
- [24] Bai, X.; Zhai, Y. B.; Zhang, Y. Green Approach to Prepare Graphene-based Composites with High Microwave Absorption Capacity. *J. Phys. Chem. C* **2011**, *115*, 11673-11677.
- [25] Wang, C. H.; He, X. D.; Shang, Y. Y.; Peng, Q. Y.; Qin, Y. Y.; Shi, E. Z.; Yang, Y. B.; Wu, S. T.; Xu, W. J.; Cao, A. Y.; Li, Y. B. Multifunctional Graphene Sheet-Nanoribbon Hybrid Aerogels. *J. Mater. Chem. A* **2014**, *2*, 14994-15000.
- [26] Wang, C. H.; Li, Y. B.; He, X. D.; Ding, Y. J.; Peng, Q. Y.; Zhao, W. Q.; Shi, E. Z.; Wu, S. T.; Cao, A. Y. Cotton-Derived Bulk and Fiber Aerogels Grafted with Nitrogen-Doped Graphene. *Nanoscale* **2014**, *7*, 7550-7558.
- [27] Wu, F.; Xia, Y. L.; Wang, Y.; Wang, M. Y. Two-step Reduction of Self-Assembled Three-Dimensional (3D) Reduced Graphene Oxide (RGO)/Zinc Oxide (ZnO) Nanocomposites for Electromagnetic Absorption. *J. Mater. Chem. A* **2014**, *2*, 20307-20315.
- [28] Zhang, H.; Xie, A. J.; Wang, C. P.; Wang, H. S.; Shen, Y. H.; Tian, X. Y. Novel rGO/ α -Fe₂O₃ Composite Hydrogel: Synthesis, Characterization and High Performance of Electromagnetic Wave Absorption. *J. Mater. Chem. A* **2013**, *1*, 8547-8552.
- [29] Liu, W. W.; Li, H.; Zeng, Q. P.; Duan, H. N.; Guo, Y. P.; Liu, X. F. Fabrication of Ultralight

- Three-Dimensional Graphene Networks with Strong Electromagnetic Wave Absorption Properties. *J. Mater. Chem. A* **2015**, *3*, 3739-3747.
- [30] Han, M. K.; Yin, X. W.; Kong, L.; Li, M.; Duan, W. Y.; Zhang, L. T.; Cheng, L. F. Graphene-wrapped ZnO Hollow Spheres with Enhanced Electromagnetic Wave Absorption Properties. *J. Mater. Chem. A* **2014**, *2*, 16403-16409.
- [31] Zhao, X. C.; Zhang, Z. M.; Wang, L. Y.; Xi, K.; Cao, Q. Q.; Wang, D. H.; Yang, Y.; Du, Y. W. Excellent Microwave Absorption Property of Graphene-coated Fe Nanocomposites. *Sci. Rep* **2013**, *3*, 3421.
- [32] Jiang, J. J.; Li, D.; Geng, D. Y.; An, J.; He, J.; Liu, W.; Zhang, Z. D. Microwave Absorption Properties of Core Double-Shell FeCo/C/BaTiO₃ Nanocomposites. *Nanoscale* **2014**, *6*, 3967-3971.
- [33] Huang, H. D.; Liu, C. Y.; Zhou, D.; Jiang, X.; Zhong, G. J.; Xiang, D.; Li, Z. M. Cellulose Composite Aerogel for Highly Efficient Electromagnetic Interference Shielding. *J. Mater. Chem. A* **2015**, *3*, 4983-4991.
- [34] Hu, C. G.; Mou, Z. Y.; Lu, G. W.; Chen, N.; Dong, Z. L.; Hu, M. J.; Qu, L. T. 3D Graphene-Fe₃O₄ Nanocomposites with High-Performance Microwave Absorption. *Phys. Chem. Chem. Phys.* **2013**, *15*, 13038-13043.



Scheme 1. Flow diagram for the fabrication of the CF@G and CF@G@PPy aerogels. a)

Cigarette filters and graphene oxide (GO) were mixed together and then dried in air followed by carbonization. Cellulose fibers were carbonized into carbon fibers (CF) and GO nanosheets were reduced into graphene nanosheets during the thermal annealing. Finally, the CF@G aerogels were coated with PPy to synthesize the CF@G@PPy aerogels. b) Photographs showing the detailed synthesis process.

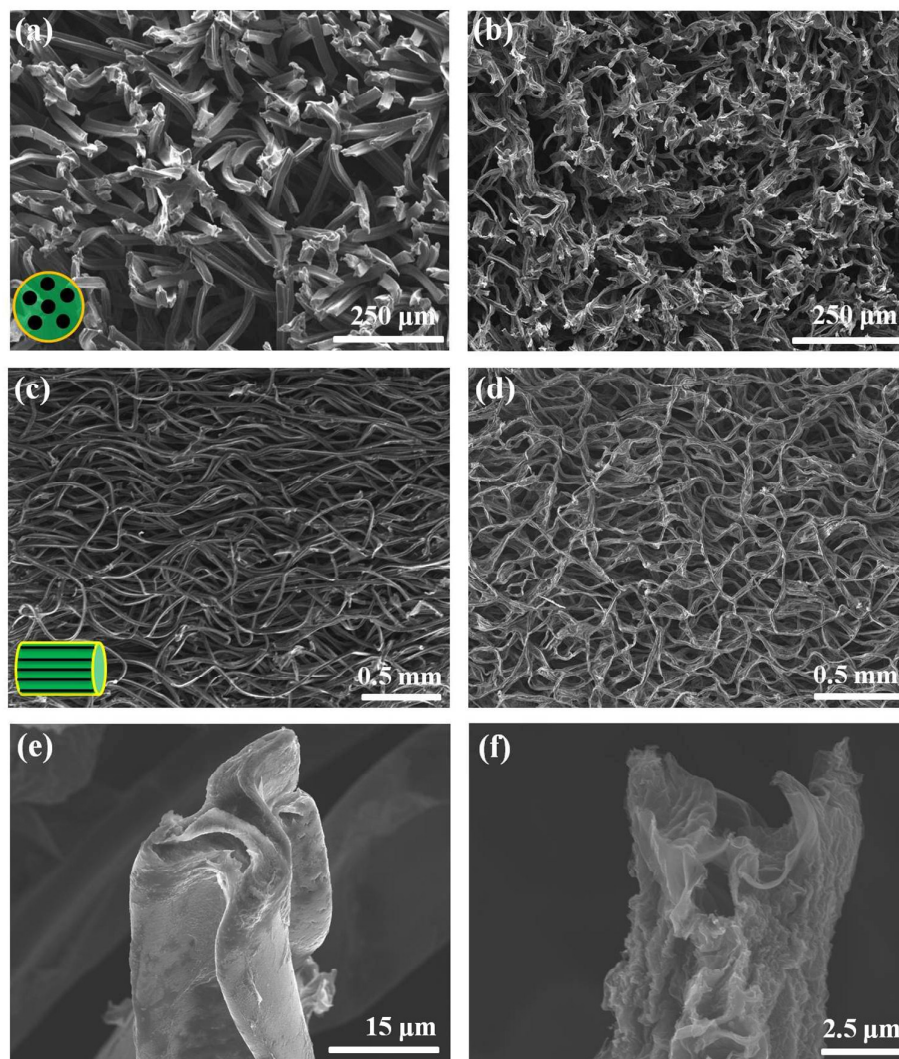


Figure 1. SEM micrographs of CA@GO and CF@G aerogels. a, b) Cross-sectional view of CA@GO and CF@G aerogels, respectively. c, d) Lateral view of CA@GO and CF@G aerogels, respectively. e, f) Amplified photos of one single fiber inside CA@GO and CF@G aerogels, respectively. Inset of a) and c) are illustrations indicating the top and side view of the sample.

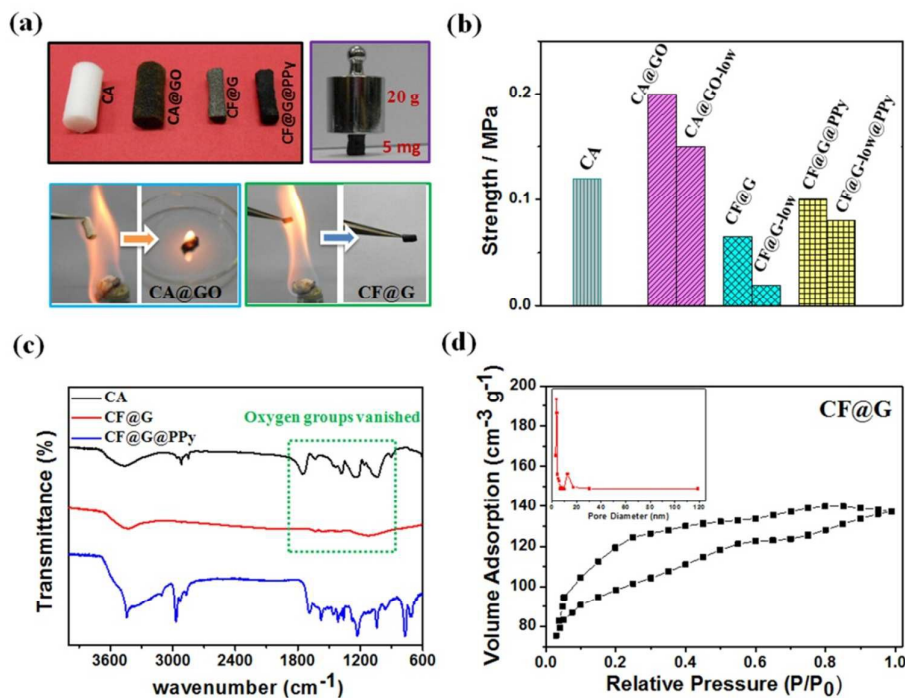


Figure 2. Mechanical properties, flame resistance and chemical characterization of CF@G aerogel. a) Photo of CA, CA@GO, CF@G and CF@G@PPy aerogel, respectively; Photo showing that a CF@G monolith of 5 mg can sustain a 20 g weight; Photo of CA@GO and CF@G burned with an alcohol burner. b) Mechanical strength of CA, CA@GO, CF@G and CF@G@PPy aerogel. GO-low indicates the sample prepared using a lower concentration (5 mg mL⁻¹) GO solution. c) FT-IR spectrum of CA, CF@G and CF@G@PPy, respectively. d) N₂ adsorption-desorption isotherms of the CF@G. Inset is the pore size distribution plots.

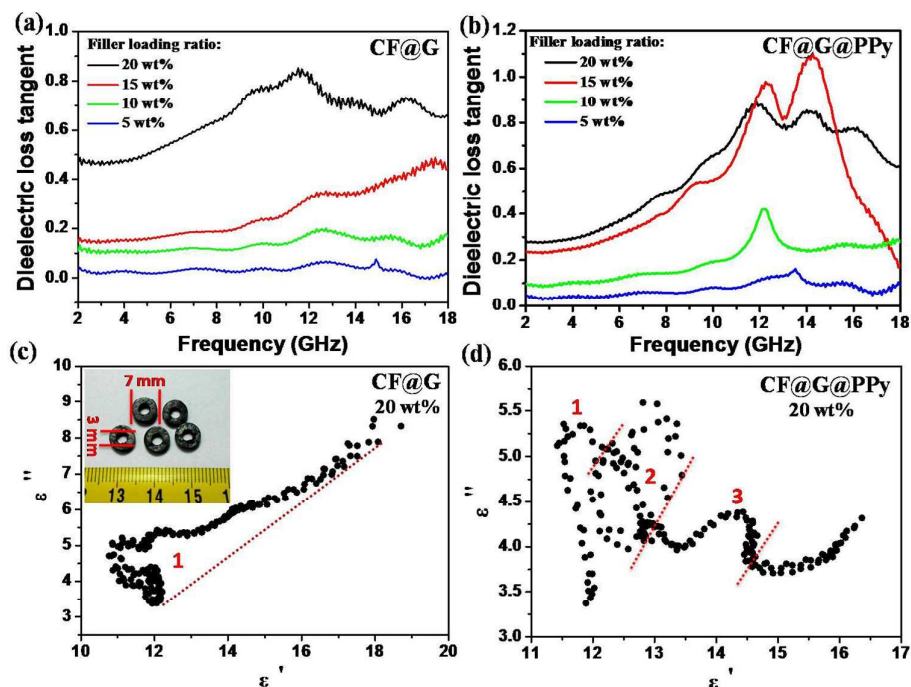


Figure 3. Dielectric dissipation factors and Cole-Cole semicircle curves of CF@G and CF@G@PPy aerogels. a, b) Dielectric dissipation factors ($\tan \delta_E$) of CF@G and CF@G@PPy aerogels with different filler loadings in paraffin wax in the frequency range of 2-18 GHz. c, d) Typical Cole-Cole semicircles (ϵ'' vs ϵ') for CF@G and CF@G@PPy aerogels with 20 wt% in paraffin wax in the frequency range of 2-18 GHz. Inset of c) is the photo of aerogels in paraffin wax with an inner diameter of 3 mm, outer diameter of 7 mm.

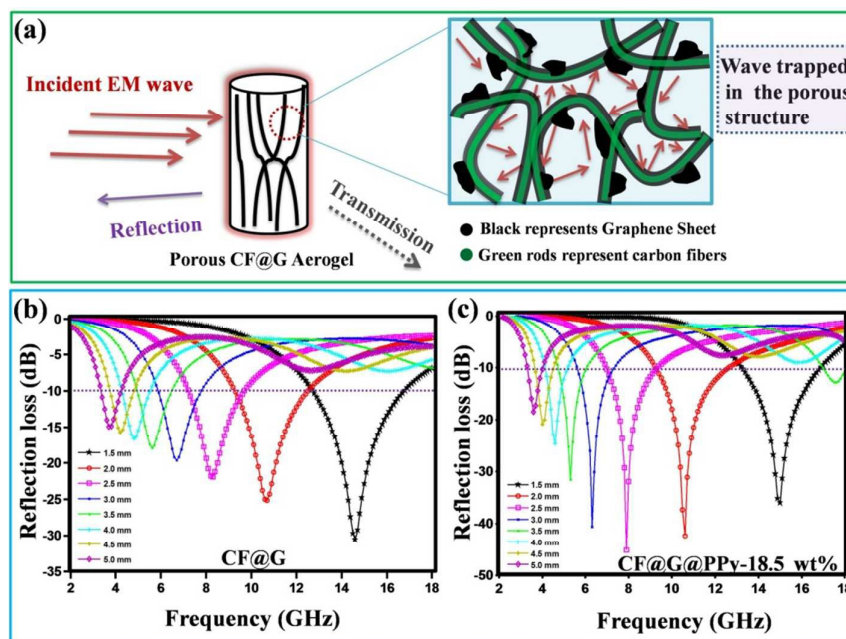


Figure 4. Absorption mechanism and EM wave reflection losses. a) Schematic illustration of the absorption mechanism. b, c) RL of CF@G and CF@G@PPy aerogels in the frequency range of 2-18 GHz. (Filler loadings of all samples are 20 wt% in wax.)

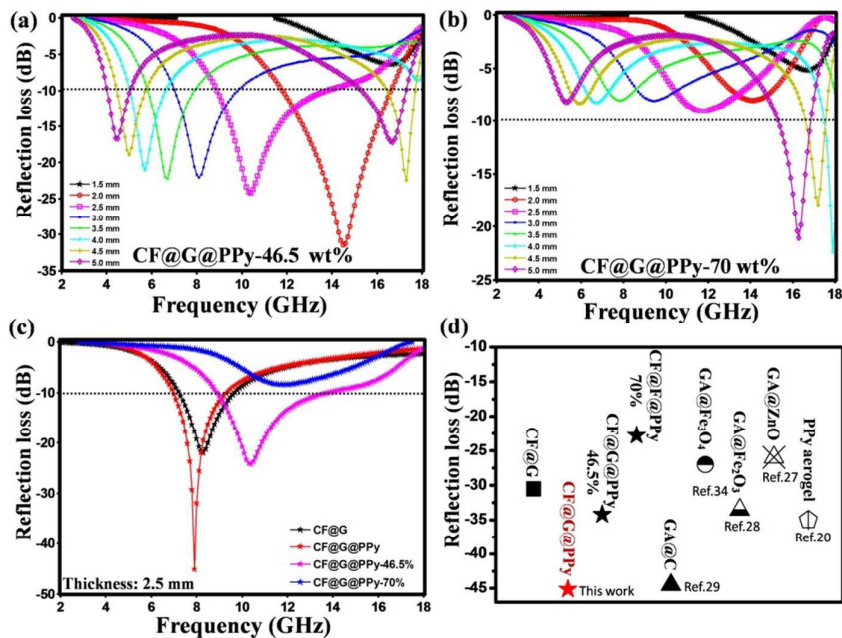
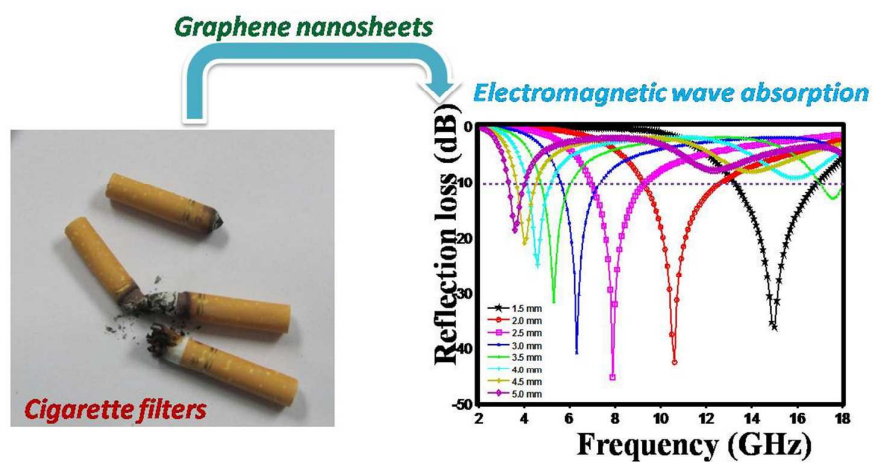


Figure 5. EM wave reflection losses of CF@G@PPy aerogels with different PPy content.

a, b) RL of CF@G@PPy aerogels with 46.5 wt% and 70 wt% PPy content in the frequency range of 2-18 GHz, respectively. c) RL of CF@G, CF@G@PPy, CF@G@PPy (46.5 wt%) and CF@G@PPy (70 wt%) samples with thickness of 2.5 mm in the frequency of 2-18 GHz. d). Comparison of minimum reflection losses (RL_m) of different samples.

Table of Contents



Graphene aerogels with excellent electromagnetic wave absorption properties are fabricated by using cigarette filters as the template via a simple dip-coating method.